

# Natural Killer Cells Are Involved in Acute Lung Immune Injury Caused by Respiratory Syncytial Virus Infection

Fengqi Li,<sup>a</sup> Hanqing Zhu,<sup>a</sup> Rui Sun,<sup>a,b</sup> Haiming Wei,<sup>a,b</sup> and Zhigang Tian<sup>a,b</sup>

Department of Immunology, School of Life Sciences, University of Science and Technology of China, Hefei, Anhui, China,<sup>a</sup> and Hefei National Laboratory for Physical Sciences at Microscale, Hefei, Anhui, China<sup>b</sup>

**It is known that respiratory syncytial virus (RSV) is the main cause of bronchiolitis and pneumonia in young children. RSV infection often leads to severe acute lung immunopathology, but the underlying immune mechanisms are not yet fully elucidated. Here, we found that RSV infection induced severe acute lung immune injury and promoted the accumulation and activation of lung natural killer (NK) cells at the early stage of infection in BALB/c mice. Activated lung NK cells highly expressed activating receptors NKG2D and CD27 and became functional NK cells by producing a large amount of gamma interferon (IFN- $\gamma$ ), which was responsible for acute lung immune injury. NK cell depletion significantly attenuated lung immune injury and reduced infiltration of total inflammatory cells and production of IFN- $\gamma$  in bronchoalveolar lavage fluid (BALF). These data show that NK cells are involved in exacerbating the lung immune injury at the early stage of RSV infection via IFN- $\gamma$  secretion.**

Human respiratory syncytial virus (RSV) is the primary cause of hospitalization in young children worldwide. RSV usually results in upper respiratory tract disease and is also associated with serious lower respiratory tract disease throughout life (6). The innate and adaptive immune systems play critical roles in the host response to infection and tissue injury during RSV infection. Recent analysis indicates that the excessive cellular immune response is thought to be involved in immunopathogenesis both in humans and in mouse models (9, 19). T cells have been demonstrated to be responsible for the lung immune injury in this process (10, 30, 33). However, in an acute infection, it remains necessary to find the immune cells responsible for the lung injury before T cells are recruited or exert their function.

Natural killer (NK) cells, members of the innate immune system in both humans and mice, play an important role in the immune response to tumor, bacterium, parasite, and virus infection (21, 26). Increasing evidence suggests that NK cells can lead to the tissue injury. For instance, NK cells activated by poly(I):poly(C) and D-galactosamine coinjection can produce gamma interferon (IFN- $\gamma$ ), causing damage to hepatocytes (14). NK cells are also the pivotal mediators during fatal *Ehrlichia*-induced toxic shock-like syndrome (27). NK cells are an important population of innate immune cells in the lung. Compared with other organs, such as spleen, lymph node, and bone marrow, there are higher percentages of NK cells in the lungs in mice (23). Thus, the aim of the present study was to investigate whether NK cells are involved in acute lung immune injury caused by RSV infection.

In this study, we observed that RSV infection induced acute lung immune injury in mice. NK cells accumulated in the lungs and activated at the early stage of RSV infection. These activated NK cells highly expressed NKG2D and CD27 and were able to produce high levels of IFN- $\gamma$  that were responsible for acute lung immune injury during RSV infection. Depletion of NK cells or neutralization of IFN- $\gamma$  could attenuate the lung immune injury. Thus, these results suggested that NK cells are involved in the lung immune injury at the early stage of RSV infection and that IFN- $\gamma$  is an important mediator in this process.

## MATERIALS AND METHODS

**Mice and virus.** Female BALB/c and SCID (BALB/c background) mice (6 to 10 weeks of age, 20 to 25 g body weight) were obtained from the Shanghai Experimental Animal Center (Chinese Academy of Sciences, Shanghai, China) and maintained at an animal facility under specific-pathogen-free conditions. Animal care and experimental procedures were performed in accordance with experimental-animal guidelines of the University of Science and Technology of China. Virus of the RSV Long strain (subtype A) were grown in Hep-2 cells, frozen at  $-80^{\circ}\text{C}$ , and assayed for infectivity. Mock-infected Hep-2 cells were used as the control. The stock of RSV consisted of  $1 \times 10^7$  PFU per ml.

**Mouse infection.** Experimental mice were anesthetized intraperitoneally (i.p.) with sodium pentobarbital (50  $\mu\text{g/g}$  of body weight) before they were infected intranasally (i.n.) with  $1 \times 10^6$  PFU of RSV in 100  $\mu\text{l}$  of stock. Control mice received 100  $\mu\text{l}$  of mock-infected Hep-2 lysate alone. At the indicated time points after RSV infection, clinical characteristics were observed and recorded. (For ruffled fur or ataxia assessments, “–” represents the absence of ruffled fur or ataxia and “+” represents the presence of ruffled fur or ataxia; for lung hyperemia assessments, “–,” “+,” and “++” represent areas of 0%, 30% to 70%, and >70% lung hyperemia, respectively.) Meanwhile, mice were monitored and body weight changes were recorded.

**Measurement IFN- $\gamma$  in BALF.** Bronchoalveolar lavage fluids (BALF) were gathered as previously described (20). In brief, sterile phosphate-buffered saline (PBS) (1 ml) was injected into the lungs of sacrificed mice, a lavage step was performed once, and then BALF samples were centrifuged at  $350 \times g$  for 5 min ( $4^{\circ}\text{C}$ ) and the supernatants were collected and kept at  $-80^{\circ}\text{C}$  until required. Levels of IFN- $\gamma$  were measured using an enzyme-linked immunosorbent assay (ELISA) kit from Senxiong Biotech (Shanghai, China).

**Isolation of BAL fluid cells and lung mononuclear cells.** BAL fluid cells were washed from the lungs with 1 ml of PBS through an intratra-

Received 3 September 2011 Accepted 5 December 2011

Published ahead of print 14 December 2011

Address correspondence to Zhigang Tian, tzg@ustc.edu.cn.

Copyright © 2012, American Society for Microbiology. All Rights Reserved.

doi:10.1128/JVI.06209-11

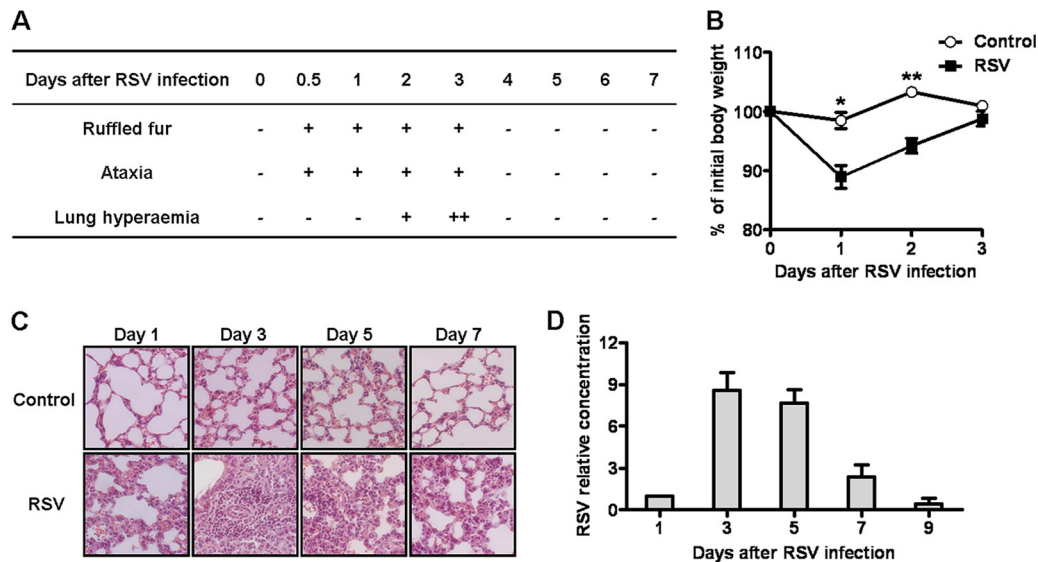


**FIG 1** RSV infection induces acute lung immune injury in mice. Female BALB/c mice were infected i.n. with  $1 \times 10^6$  PFU of RSV. (A and B) Clinical characteristics (A) and body weight changes (B) of mice were measured after RSV infection. (C) Lung histology were determined by hematoxylin and eosin (H&E) staining (original magnification,  $\times 200$ ) at the indicated times after RSV infection. (D) RSV loads in the lungs were detected by real-time quantitative PCR at the indicated times after RSV infection. \*,  $P < 0.05$ ; \*\*,  $P < 0.01$ .

cheal cannula. Cell viability was determined by trypan blue exclusion. After centrifugation, the pellet was resuspended and the cell numbers were counted. Lung mononuclear cells were isolated as previously described with minor modifications (17). Briefly, mice were sacrificed and exsanguinated. The lungs were excised and minced and then digested for 60 min at  $37^\circ\text{C}$  in a swing bed with RPMI 1640 containing 0.1% collagenase I (Sigma) and 5% fetal calf serum. The large pieces of lung were removed by filtration through gauze. The mononuclear cells were prepared by density gradient centrifugation with 40% and 70% Percoll (GE Healthcare). Cells were collected from the 40%-70% Percoll interface, washed twice, and counted.

**Lung histopathology.** For histological analysis, lung tissue was removed and fixed immediately in 10% neutral-buffered formalin–PBS for more than 24 h, embedded in paraffin, and cut into  $5\text{-}\mu\text{m}$ -thick sections. The sections were deparaffinized and stained with hematoxylin and eosin to determine histological changes.

**Determination of viral loads.** Viral loads were determined by real-time quantitative PCR after RSV infection. Briefly, total RNA was extracted from whole-lung tissue and then cDNA was synthesized. Primers specific for the nucleocapsid (N) gene of RSV were used (forward, 5'-GGAACAAGTTGTTGAGGTTTATGAATATGC-3'; reverse, 5'-CTTCTGCTGTCAAGTCTAGTACTGTAGT-3') (2). The viral loads in each sample were calculated by relative quantification. Real-time PCR were performed with SYBR Premix Ex *Taq* according to the instructions of the manufacturer (Takara). The ratio of viral RNA to mouse  $\beta$ -actin mRNA in wild-type (WT) BALB/c mice at day 1 after RSV infection was used as a control. The primers for mouse  $\beta$ -actin were used (forward, 5'-TGACGTTGACATCCGTAAGACC-3'; reverse, 5'-CTCAGGAGGAGCAATGATCTTGA-3'). All primers were synthesized by Sangon Biotech (Shanghai, China).

**Neutralization of IFN- $\gamma$  *in vivo*.** Mice were treated intravenously (i.v.) with rat anti-mouse IFN- $\gamma$  monoclonal antibodies (MAbs) (100  $\mu\text{g}$  per mouse) for IFN- $\gamma$  neutralization *in vivo* (rat IgG1,  $\kappa$  as the control) 24 h before and 48 h after an inoculation of  $1 \times 10^6$  PFU of RSV was administered. Rat anti-mouse IFN- $\gamma$  monoclonal antibodies (R4-6A2) and rat IgG1,  $\kappa$  (isotype control) were purchased from eBioscience.

**NK cell depletion.** Mice were treated i.v. with rabbit anti-mouse asialo-GM-1 (AsGM-1) antibodies (50  $\mu\text{g}$  per mouse) for NK cell deple-

tion (normal rabbit serum as the control) 24 h before and 48 h after an inoculation of  $1 \times 10^6$  PFU of RSV was administered. The effects of the NK cell depletion in lung, spleen, and liver tissue were confirmed by flow cytometry assay 24 h after the primary anti-AsGM-1 injection. Rabbit anti-mouse AsGM-1 antibodies were purchased from Wako Co., Ltd. (Tokyo, Japan).

**Flow cytometry assay.** After blocking the Fc receptor with anti-CD16/CD32, single-cell suspensions were incubated with the fluorescently labeled monoclonal antibodies (MAbs) at  $4^\circ\text{C}$  for 30 min in PBS (containing 0.1% sodium azide and 1% bovine serum albumin [BSA]) and then washed twice. For intracellular cytokine staining, cells were stimulated for 4 h at  $37^\circ\text{C}$  with phorbol myristate acetate (PMA) (40 ng/ml), ionomycin (1  $\mu\text{g}/\text{ml}$ ), and monensin (10  $\mu\text{g}/\text{ml}$ ) (all from Sigma); after extracellular markers were stained, cells were fixed, permeabilized, and stained with phycoerythrin (PE)–anti-IFN- $\gamma$  or the isotype control. Samples were analyzed using BD FACScalibur and FlowJo software. Cells were gated according to forward scatter and side scatter, and cell types were identified by phenotype as follows: for NK cells,  $\text{CD}3^- \text{DX}5^+$ ; and for T cells,  $\text{CD}3^+ \text{DX}5^-$ . The anti-mouse MAbs used for flow cytometry included the following: anti-mouse CD16/CD32; fluorescein isothiocyanate (FITC)-conjugated anti-CD49b (clone DX5) and FITC-rat IgM,  $\kappa$  (isotype control for anti-CD49b); PE-conjugated anti-CD69 (clone H1.2F3), anti-NKG2D (clone CX5), anti-CD27 (clone LG.3A10), anti-IFN- $\gamma$  (clone XMG1.2), anti-NKp46 (clone 29A1.4), PE-Armenian hamster IgG1,  $\lambda 3$  (isotype control for anti-CD69), PE-rat IgG1,  $\kappa$  (isotype control for anti-NKG2D and anti-IFN- $\gamma$ ), PE-Armenian hamster IgG1,  $\kappa$  (isotype control for anti-CD27), and PE-rat IgG2a,  $\kappa$  (isotype control for anti-NKp46); and PE-CY5-conjugated anti-CD3 $\epsilon$  (clone 145-2C11), PE-CY5-Armenian hamster IgG1,  $\kappa$  (isotype control for anti-CD3 $\epsilon$ ). All the antibodies were purchased from BD Biosciences.

**Statistical analysis.** Student's *t* tests were used for statistical analyses. The experimental data were expressed as means  $\pm$  standard errors of the means (SEMs), and the data are representative of the results of two to three independent experiments.  $P < 0.05$  was considered statistically significant.

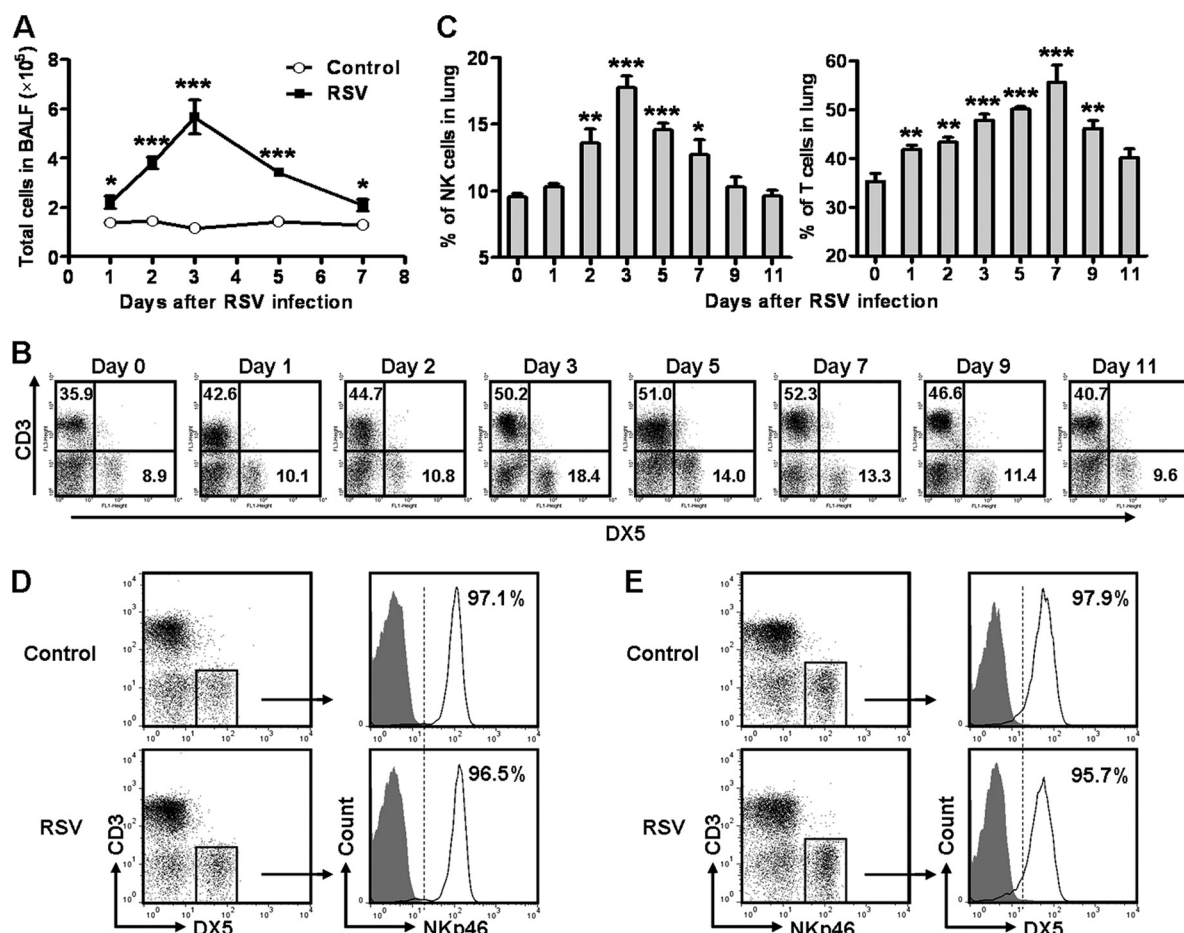


**FIG 2** RSV infection induces lung immune responses in mice. Female BALB/c mice were infected i.n. with  $1 \times 10^6$  PFU of RSV. (A) Cell numbers in BALF were calculated. (B) Lung mononuclear cells were labeled with anti-mouse CD3 and DX5, and percentages were determined by flow cytometry assay at the indicated times after RSV infection. x axis, FL-1 height; y axis, FL-3 height. (C) Percentages of NK cells (CD3<sup>-</sup>, DX5<sup>+</sup>) and T cells (CD3<sup>+</sup> DX5<sup>-</sup>). (D and E) At day 2 after RSV infection, lung mononuclear cells were labeled with anti-mouse CD3, DX5, and NKp46 and determined by flow cytometry assay. (D) Expression of NKp46 on CD3<sup>-</sup> DX5<sup>+</sup> cells. (E) Expression of DX5 on CD3<sup>-</sup> NKp46<sup>+</sup> cells. \*,  $P < 0.05$ ; \*\*,  $P < 0.01$ ; \*\*\*,  $P < 0.001$ .

## RESULTS

**RSV infection induces acute lung immune injury in mice.** As observed previously (5), RSV intranasal infection led to significant clinical characteristics in female BALB/c mice. Ruffled fur and ataxia occurred at 12 h and continued for 3 days after infection. Meanwhile, lung hyperemia occurred at day 2 and reached a peak at day 3 after RSV infection (Fig. 1A). Furthermore, compared with control mice, RSV-infected mice showed significant weight loss at days 1 and 2 after infection, and the body weight returned to normal levels at day 3 (Fig. 1B). The analysis of lung histology showed that there were lots of inflammatory cells infiltrating into the lungs and distributing into peribronchiolar space at day 3 and that the mice recovered from this condition at days 5 and 7 (Fig. 1C). Determination of viral loads in the lungs of RSV-infected mice revealed that the viral loads gradually increased from day 1 to day 3 and then decreased (Fig. 1D). Together, these results suggested that RSV could induce severe lung immune injury at the early stage of infection in mice.

**Lung NK cells are activated by RSV infection.** Infiltration of inflammatory cells plays a critical role in RSV-induced illness (30). We next explored which cells were involved in the acute lung

immune injury at the early stage of RSV infection. Compared with control mice, the total number of cells in BALF of RSV-infected mice increased and reached a peak at day 3 and then returned to nearly normal levels at day 7 after RSV infection (Fig. 2A). Previous studies have observed that NK cells play crucial roles in the elimination of virus at the early stage of infection but also that they are an important contributor to virus-induced lung immune injury (1, 8). We found that during RSV infection, the percentages of NK (CD3<sup>-</sup> DX5<sup>+</sup>) and T (CD3<sup>+</sup> DX5<sup>-</sup>) cells in the lungs were increased, and the percentage of NK cells reached a peak at day 3, but the percentage of T cells reached a peak at day 7 (Fig. 2B and C). To further confirm the marker of the NK cell population, we detected the expression of CD3, DX5, and NKp46 on lung lymphocytes in uninfected mice and mice infected with RSV for 2 days. We found that most of the CD3<sup>-</sup> DX5<sup>+</sup> cells expressed NKp46 (>95%) and most of the CD3<sup>-</sup> NKp46<sup>+</sup> cells expressed DX5 (>95%) regardless of the presence or absence of RSV infection (Fig. 2D and E). Thus, CD3<sup>-</sup> DX5<sup>+</sup> cells in the lungs can represent the CD3<sup>-</sup> NKp46<sup>+</sup> cell populations that have been considered to represent NK cells in mice. Next, we examined the activation of NK and T cells by detecting CD69, an inducible surface



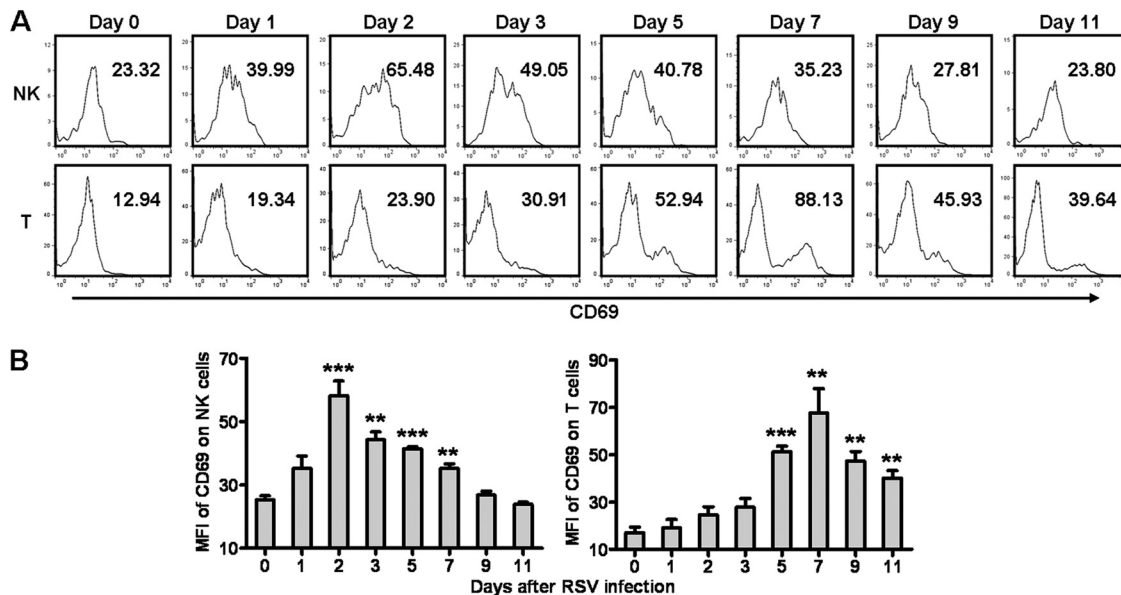


**FIG 3** Lung NK cells and T cells are activated after RSV infection. Female BALB/c mice were infected i.n. with  $1 \times 10^6$  PFU of RSV. (A) At days 0, 1, 2, 3, 5, 7, 9, and 11 after RSV infection, the expression of CD69 on NK cells ( $CD3^- DX5^+$ ) and T cells ( $CD3^+ DX5^-$ ) was detected by flow cytometry assay. (B) Numbers inside the histogram represent mean fluorescence intensity (MFI) levels of CD69 on NK cells and T cells. \*\*,  $P < 0.01$ ; \*\*\*,  $P < 0.001$ .

marker for activated lymphocytes (35). We found that the expression of CD69 on NK cells was increased and reached a peak at day 2, while the expression of CD69 on T cells was increased and reached a peak at day 7 (Fig. 3). Together, these results indicated that NK cells were recruited and activated earlier than T cells and that they might be the main contributor to acute lung immune injury at the early stage of RSV infection.

**RSV infection upregulates the expression of NKG2D and CD27 on lung NK cells.** NK cells can promote tissue immune injury through NKG2D, an activating receptor on NK cells, during viral infection (3, 32). In addition, CD27 is a costimulated molecule and can be upregulated on NK cells after viral infection, and  $CD27^+$  NK cells have a stronger function with respect to cytokine secretion and cytotoxicity (7, 13, 29). Thus, we measured the expression of NKG2D and CD27 on NK cells within 72 h after RSV infection. We found that the percentages of  $NKG2D^+$  and  $CD27^+$  NK cells were increased and reached a peak at 48 h after RSV infection (Fig. 4). Therefore, these results suggested that NK cells activated by RSV infection exerted a strong function with respect to secretion of cytokines and killing of target cells and that they might also be responsible for lung immune injury.

**NK cell-derived  $IFN-\gamma$  is involved in acute lung immune injury during RSV infection.** Recent analysis indicates that the pro-inflammatory cytokine storm is a major contributor to lung injury and death during respiratory viral infection, and  $IFN-\gamma$ , as a member of the cytokine storm, plays a critical role in this process (15). In our study, the levels of  $IFN-\gamma$  in BALF were increased and reached a peak at day 3 after RSV infection (Fig. 5A). It has been noted that the NK cell is the main source of  $IFN-\gamma$  at the early stage of viral infection (16, 28). In our study, we found that RSV infection could improve the ability of NK cells to produce  $IFN-\gamma$ , and the proportion of  $IFN-\gamma$ -positive NK cells in the lungs was also increased (Fig. 5B and C). Combining these results with previous results, we found that the phases of the production of  $IFN-\gamma$ , the increase of NK cells, and the immune injury of lung tissue pro-

ceeded in parallel (Fig. 1 and 2). Thus, we presumed that NK cells were involved in the lung immune injury at the early stage of RSV infection through  $IFN-\gamma$  secretion. To confirm the role of  $IFN-\gamma$  in the lung immune injury induced by RSV infection, we neutralized  $IFN-\gamma$  *in vivo* by anti- $IFN-\gamma$  injection 24 h before and 48 h after RSV infection (Fig. 5D) and found that, compared with control mice, anti- $IFN-\gamma$ -treated mice displayed less inflammatory cell infiltration in the lungs (Fig. 5E), though higher viral loads were detected in the lungs (Fig. 5F) at day 3 after RSV infection. Together, these results indicated that NK cell-derived  $IFN-\gamma$  is involved in acute lung immune injury during RSV infection.

**Depletion of NK cells attenuates acute lung immune injury caused by RSV infection.** To validate the role of NK cells in lung immune injury at the early stage of RSV infection, we depleted NK cells by anti-AsGM-1 injection 24 h before and 48 h after RSV infection (Fig. 6A) and observed that there were fewer lung, spleen, and liver NK cells in anti-AsGM-1-treated BALB/c mice 24 h after primary injection compared with control mice (Fig. 6B). In this study, we found that, compared with control mice, NK cell-depleted BALB/c mice displayed less body weight loss at days 1 and 2 after RSV infection (Fig. 6C) and less inflammatory cell infiltration in the lungs at day 3 after RSV infection (Fig. 6D). Meanwhile, the viral loads in the lungs were increased in NK cell-depleted mice at day 3 after RSV infection (Fig. 6E). Furthermore, the total numbers of cells and the levels of  $IFN-\gamma$  in BALF at day 3 after RSV infection were also decreased in NK cell-depleted mice (Fig. 6F and G). Previous studies have found that AsGM-1 is expressed by T cells in viral infection and by NK cells (22). Thus, anti-AsGM-1 could deplete NK cells but could also deplete other cell populations. To further confirm the role of NK cells, we next used SCID mice with a BALB/c background, which lack T cells and B cells. We depleted NK cells by anti-AsGM-1 injection 24 h before and 48 h after RSV infection in SCID mice. At day 3 after RSV infection, we also found that NK cell-depleted SCID mice displayed less inflammatory cell infiltration in the lungs (Fig. 6H) and that higher viral

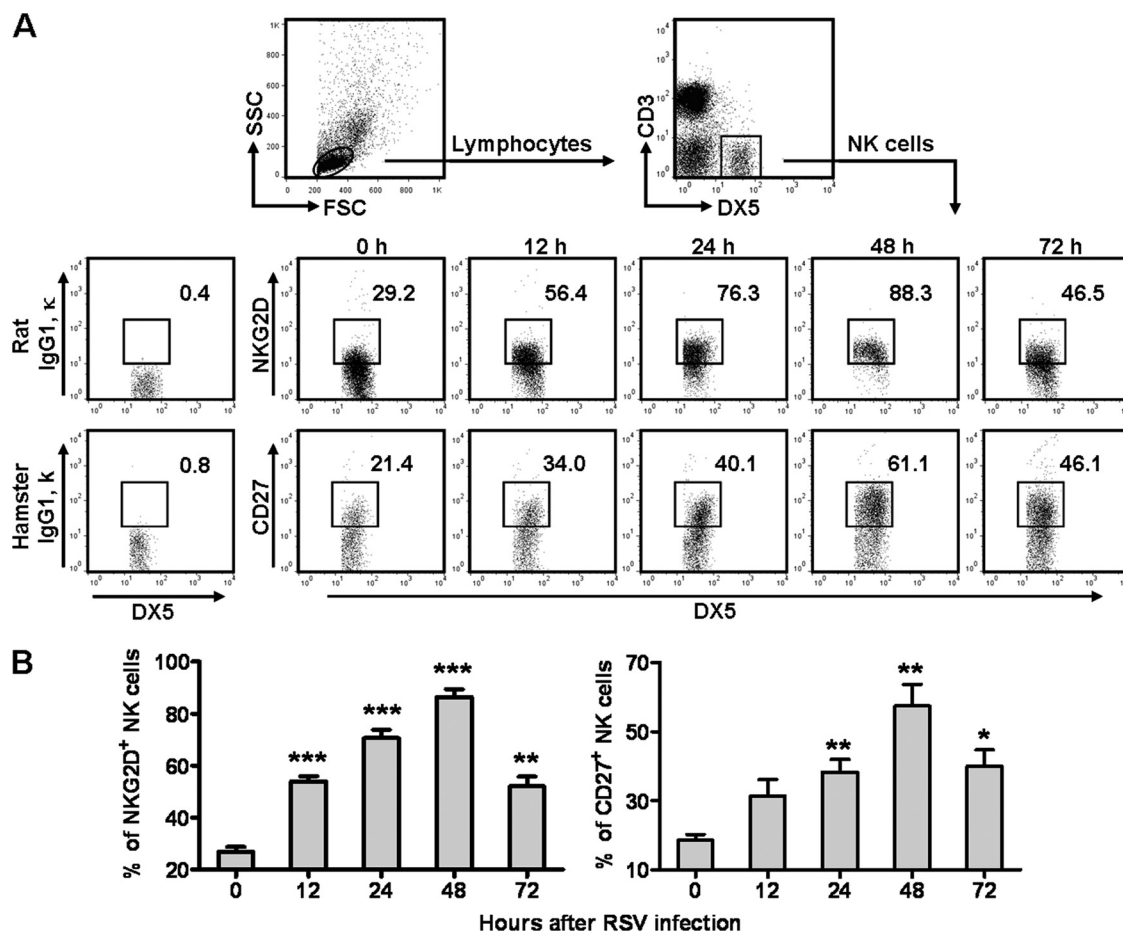


**FIG 4** RSV infection upregulates the expression of NKG2D and CD27 on lung NK cells. Female BALB/c mice were infected i.n. with  $1 \times 10^6$  PFU of RSV. (A) After RSV infection, expression of NKG2D and CD27 on lung NK cells ( $CD3^- DX5^+$ ) was detected by flow cytometry assay at the indicated times. (B) Percentages of NKG2D<sup>+</sup> and CD27<sup>+</sup> NK cells. \*,  $P < 0.05$ ; \*\*,  $P < 0.01$ ; \*\*\*,  $P < 0.001$ .

loads were detected in the lungs (Fig. 6I). Therefore, these results suggested that NK cells were indeed involved in acute lung immune injury at the early stage of RSV infection and that IFN- $\gamma$  was an important mediator in this process.

## DISCUSSION

RSV, a single-stranded negative-sense RNA virus of the Paramyxoviridae family, is the chief cause of bronchiolitis and viral pneumonia in younger children (9). The bronchiolitis and pneumonia induced by RSV infection have been believed to be immunopathological in nature, because a large number of inflammatory cells are accumulated and activated in the lungs after infection (4, 24). As reported previously by others, T cells are the main inflammatory infiltrates and responsible for lung immune injury during RSV infection because T cells are recruited into the lung after 7 days following RSV infection and promote inflammation and hamper the recruitment of regulatory T cells (25, 31). In this study, we found that RSV infection induced severe acute lung immune injury at the early stage of infection (day 3) and that the mice recovered from the immune injury 7 days after RSV infection in our mouse model, which differs from observations described previously (10, 11, 33). The discrepancy might be attributable to the use of different RSV

strains: we used the Long strain, but others used the A2 strain. At the early stage of RSV infection, though T cells started to be recruited, the percentages of total T cells and activated T were relatively low (Fig. 2 and 3). However, in our study, the lung immune injury during RSV infection happened within 72 h, and the T cell effector function is not expected to begin in the early stage. Therefore, it is possible that other early response immune cells rather than T cells take part in RSV-mediated acute lung immune injury.

The lung is a major entry point for pathogens into the body. Thus, rapid and effective innate immune responses are required to prevent pathogen infection and to limit their spread in the lungs. NK cells are large granular lymphocytes of the innate immune system and make up 10% of resident lymphocytes in the lung, which participate in the early control of pathogen infection and cancer and prime subsequent adaptive immune responses. However, early excessive NK cell responses also lead to immunopathology (23). In this study, the number and percentage of NK cells in the lungs began to significantly increase at 72 h after RSV infection, and most of the NK cells were in the active state. Recently, Kaiko et al. demonstrated that NK cell deficiency during RSV infection results in the suppression of IFN- $\gamma$  production by T cells and the development of a Th2 immune response and subsequent

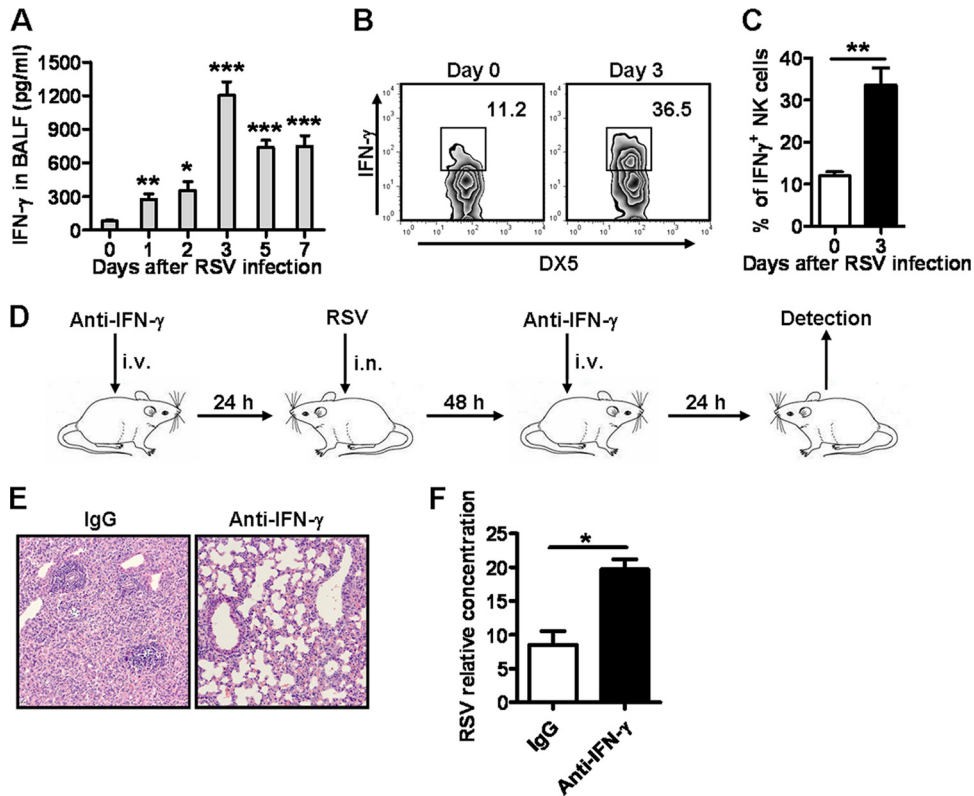


**FIG 5** NK cell-derived IFN- $\gamma$  is involved in acute lung immune injury during RSV infection. Female BALB/c mice were infected i.n. with  $1 \times 10^6$  PFU of RSV. (A) IFN- $\gamma$  levels in BALF were detected by ELISA at the indicated times after RSV infection. (B) Expression of IFN- $\gamma$  in lung NK cells (CD3<sup>-</sup>DX5<sup>+</sup>) was detected by intracellular cytokine staining at the indicated times. (C) Percentages of IFN- $\gamma$ <sup>+</sup> NK cells. (D to F) Female BALB/c mice were treated i.v. with 100  $\mu$ g of rat anti-mouse IFN- $\gamma$  MAb for IFN- $\gamma$  neutralization *in vivo* (rat IgG1,  $\kappa$  as control) 24 h before and 48 h after infection with RSV at  $1 \times 10^6$  PFU. (E and F) At day 3 after infection, lung histology was determined by H&E staining (original magnification,  $\times 200$ ) (E) and RSV loads in the lungs were detected by real-time quantitative PCR (F). \*,  $P < 0.05$ ; \*\*,  $P < 0.01$ ; \*\*\*,  $P < 0.001$ .

allergic lung disease (18). In contrast to that research, acute lung immune injury occurred at the early stage of RSV infection in our study and mice recovered at day 7 after infection. So, although an early NK cell response can prevent Th2 immune response-induced lung immune injury, the NK cell response also leads to immune injury. In fact, NK cells can play a dual role in viral infection: protecting against virus and inducing injury. In our study, we found that the virus loads were increased in both NK cell-depleted BALB/c mice and SCID mice, though the immune injury was attenuated in the lungs of these mice (Fig. 6E and I).

Mature mouse NK cells can be subdivided into CD27<sup>hi</sup> and CD27<sup>lo</sup> subsets based on the expression of CD27. CD27<sup>hi</sup> NK cells possess a stronger ability to secrete cytokines and induce cytotoxicity than CD27<sup>lo</sup> NK cells. Because CD27<sup>lo</sup> NK cells express the highly inhibitory receptors Ly49 and KLRG1, their cytotoxic activities are more tightly regulated than those of the CD27<sup>hi</sup> NK cells (12). In this study, the proportion of the CD27<sup>hi</sup> NK cells increased following RSV infection. Therefore, at the early stage of acute RSV infection, there were large amounts of CD27<sup>hi</sup> NK cells in the lungs that could induce severe acute lung injury by secreting proinflammatory cytokines and inducing cytotoxicity. During the NK cell immune response, activating receptor NKG2D is critical for the activation of NK cells and NKG2D downregulation can impair the NK cell response in respiratory infection (34). In this study, RSV infection markedly promoted the expression of

NKG2D on NK cells, and then NKG2D-ligand recognition would promote the activation of NK cells.

NK cells can act through direct and indirect pathways to mediate tissue immune injury (12). NK cells regulate the immune responses of multiple immune cells through a combination of cell surface receptors and cytokines. For example, NK cells promote the maturation and activation of dendritic cells (DCs), macrophages, and T cells (32). In this process, NK cell-derived IFN- $\gamma$ , which can promote activation of DCs, macrophages, and T cells, plays a crucial role. In this study, RSV infection promoted the production of IFN- $\gamma$  by NK cells, and at the same time, the number of T cells also increased. Therefore, IFN- $\gamma$ -induced activation of T cells might be involved in acute lung injury during RSV infection. Furthermore, depletion of NK cells and neutralization of IFN- $\gamma$  *in vivo* resulted in the attenuation of lung injury during RSV infection, which further illustrates that NK cells and IFN- $\gamma$  were involved in the RSV infection-induced acute lung injury.

In summary, the present work suggests that lung NK cells may recognize RSV-infected cells through NKG2D and its ligand and, at the same time, produce IFN- $\gamma$  that may cause damage to RSV-infected cells, thus inducing acute lung immune injury at the early stage of RSV infection (Fig. 7). Taken together, our findings may provide insight into excessive innate

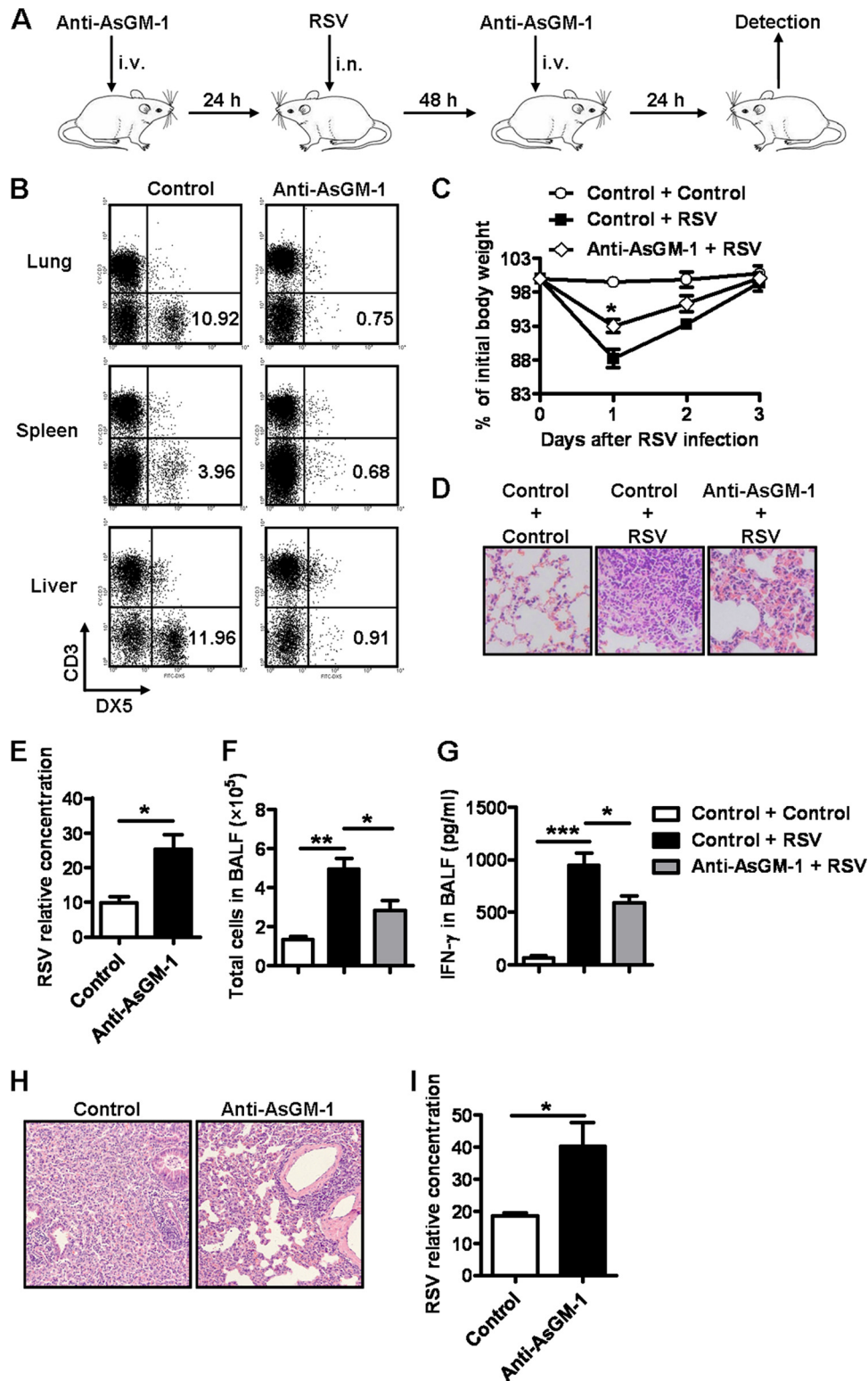


**FIG 6** Depletion of NK cells attenuates acute lung immune injury caused by RSV infection. (A) Mice were treated i.v. with 50  $\mu$ g of rabbit anti-mouse AsGM-1 for NK cell depletion (normal rabbit serum as control) 24 h before and 48 h after infection with RSV at  $1 \times 10^6$  PFU. (B) At 24 h after primary anti-AsGM-1 treatment, the effects of the NK cell depletion in lung, spleen, and liver tissue from BALB/c mice were detected by flow cytometry assay; percentages of NK cells (CD3<sup>+</sup> DX5<sup>+</sup>) are shown. (C to G) Body weight changes in NK cell-depleted BALB/c mice were measured at the indicated times (C), and at day 3 after infection, lung histology was determined by H&E staining (original magnification,  $\times 200$ ) (D), RSV loads in the lungs were detected by real-time quantitative PCR (E), cell numbers in BALF were calculated (F), and IFN- $\gamma$  levels in BALF were detected by ELISA (G). (H and I) Using samples from NK cell-depleted SCID mice, lung histology were determined by H&E staining (original magnification,  $\times 200$ ) (H) and RSV loads in the lungs were detected by real-time quantitative PCR at day 3 after infection (I). \*,  $P < 0.05$ ; \*\*,  $P < 0.01$ ; \*\*\*,  $P < 0.001$ .



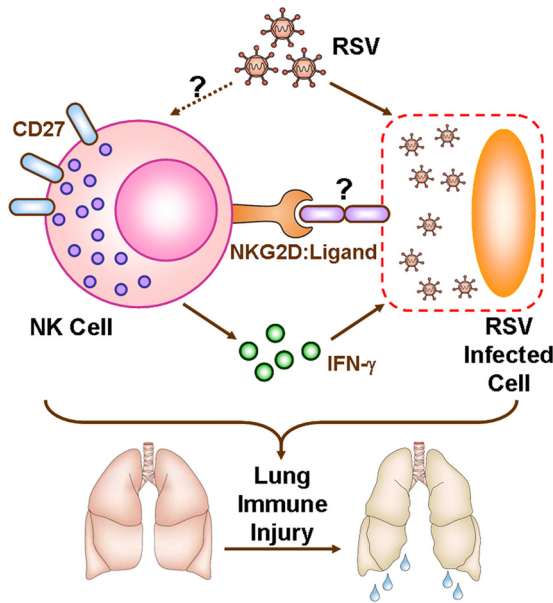


**FIG 7** Working model of NK cell-mediated acute lung immune injury during RSV infection. RSV infection promotes activation of lung NK cells, which highly express CD27 and become functional NK cells. At the same time, expression of activating NK cell receptor NKG2D upregulates and may recognize its ligand, which is expressed on RSV-infected cells. Furthermore, NK cell-derived IFN- $\gamma$  induces RSV-infected cell damage, which may lead to acute lung immune injury at the early stage of RSV infection.

immune response during respiratory infection, which is critical in lung immunopathology.

#### ACKNOWLEDGMENTS

This work was supported by the Natural Science Foundation of China (grants 31021061 and 30911120480).

We thank Jinsheng He (Department of Immunology, Anhui Medical University) for providing the Long strain of RSV.

#### REFERENCES

- Adler H, et al. 1999. In the absence of T cells, natural killer cells protect from mortality due to HSV-1 encephalitis. *J. Neuroimmunol.* 93:208–213.
- Cane PA, Pringle CR. 1991. Respiratory syncytial virus heterogeneity during an epidemic: analysis by limited nucleotide sequencing (SH gene) and restriction mapping (N gene). *J. Gen. Virol.* 72(Pt. 2):349–357.
- Chen Y, et al. 2007. Increased susceptibility to liver injury in hepatitis B virus transgenic mice involves NKG2D-ligand interaction and natural killer cells. *Hepatology* 46:706–715.
- Collins PL, Graham BS. 2008. Viral and host factors in human respiratory syncytial virus pathogenesis. *J. Virol.* 82:2040–2055.
- Davis IC, Sullender WM, Hickman-Davis JM, Lindsey JR, Matalon S. 2004. Nucleotide-mediated inhibition of alveolar fluid clearance in BALB/c mice after respiratory syncytial virus infection. *Am. J. Physiol. Lung Cell. Mol. Physiol.* 286:L112–L120.
- Dawson-Caswell M, Muncie HL, Jr. 2011. Respiratory syncytial virus infection in children. *Am. Fam. Physician* 83:141–146.
- De Colvenaer V, et al. 2011. CD27-deficient mice show normal NK-cell differentiation but impaired function upon stimulation. *Immunol. Cell Biol.* 89:803–811.
- Dotta F, et al. 2007. Coxsackie B4 virus infection of beta cells and natural killer cell insulinitis in recent-onset type 1 diabetic patients. *Proc. Natl. Acad. Sci. U. S. A.* 104:5115–5120.
- Durbin JE, Durbin RK. 2004. Respiratory syncytial virus-induced immunoprotection and immunopathology. *Viral Immunol.* 17:370–380.
- Fulton RB, Meyerholz DK, Varga SM. 2010. Foxp3+ CD4 regulatory T cells limit pulmonary immunopathology by modulating the CD8 T cell response during respiratory syncytial virus infection. *J. Immunol.* 185:2382–2392.
- Harker JA, et al. 2010. Interleukin 18 coexpression during respiratory syncytial virus infection results in enhanced disease mediated by natural killer cells. *J. Virol.* 84:4073–4082.
- Hayakawa Y, Huntington ND, Nutt SL, Smyth MJ. 2006. Functional subsets of mouse natural killer cells. *Immunol. Rev.* 214:47–55.
- Hayakawa Y, Smyth MJ. 2006. CD27 dissects mature NK cells into two subsets with distinct responsiveness and migratory capacity. *J. Immunol.* 176:1517–1524.
- Hou X, Zhou R, Wei H, Sun R, Tian Z. 2009. NKG2D-retinoic acid inducible-1 recognition between natural killer cells and Kupffer cells in a novel murine natural killer cell-dependent fulminant hepatitis. *Hepatology* 49:940–949.
- Huang KJ, et al. 2005. An interferon-gamma-related cytokine storm in SARS patients. *J. Med. Virol.* 75:185–194.
- Hussell T, Openshaw PJ. 1998. Intracellular IFN-gamma expression in natural killer cells precedes lung CD8+ T cell recruitment during respiratory syncytial virus infection. *J. Gen. Virol.* 79(Pt. 11):2593–2601.
- Ishikawa E, Nakazawa M, Yoshinari M, Minami M. 2005. Role of tumor necrosis factor-related apoptosis-inducing ligand in immune response to influenza virus infection in mice. *J. Virol.* 79:7658–7663.
- Kaiko GE, Phipps S, Angkasekwinai P, Dong C, Foster PS. 2010. NK cell deficiency predisposes to viral-induced Th2-type allergic inflammation via epithelial-derived IL-25. *J. Immunol.* 185:4681–4690.
- Krishnan S, Halonen M, Welliver RC. 2004. Innate immune responses in respiratory syncytial virus infections. *Viral Immunol.* 17:220–233.
- Li R, et al. 2010. Attenuated Bordetella pertussis protects against highly pathogenic influenza A viruses by dampening the cytokine storm. *J. Virol.* 84:7105–7113.
- Miller JS. 2002. Biology of natural killer cells in cancer and infection. *Cancer Invest.* 20:405–419.
- Moore ML, Chi MH, Goleniewska K, Durbin JE, Peebles RS, Jr. 2008. Differential regulation of GM1 and asialo-GM1 expression by T cells and natural killer (NK) cells in respiratory syncytial virus infection. *Viral Immunol.* 21:327–339.
- Morris MA, Ley K. 2004. Trafficking of natural killer cells. *Curr. Mol. Med.* 4:431–438.
- Openshaw PJ, Tregoning JS. 2005. Immune responses and disease enhancement during respiratory syncytial virus infection. *Clin. Microbiol. Rev.* 18:541–555.
- Ruckwardt TJ, Bonaparte KL, Nason MC, Graham BS. 2009. Regulatory T cells promote early influx of CD8+ T cells in the lungs of respiratory syncytial virus-infected mice and diminish immunodominance disparities. *J. Virol.* 83:3019–3028.
- Shereck E, Satwani P, Morris E, Cairo MS. 2007. Human natural killer cells in health and disease. *Pediatr. Blood Cancer* 49:615–623.
- Stevenson HL, Estes MD, Thirumalapura NR, Walker DH, Ismail N. 2010. Natural killer cells promote tissue injury and systemic inflammatory responses during fatal Ehrlichia-induced toxic shock-like syndrome. *Am. J. Pathol.* 177:766–776.
- Sun R, Gao B. 2004. Negative regulation of liver regeneration by innate immunity (natural killer cells/interferon-gamma). *Gastroenterology* 127:1525–1539.
- Takeda K, et al. 2000. CD27-mediated activation of murine NK cells. *J. Immunol.* 164:1741–1745.
- Tregoning JS, et al. 2010. The chemokine MIP1 $\alpha$ /CCL3 determines pathology in primary RSV infection by regulating the balance of T cell populations in the murine lung. *PLoS One* 5:e9381.
- Tregoning JS, Yamaguchi Y, Harker J, Wang B, Openshaw PJ. 2008. The role of T cells in the enhancement of respiratory syncytial virus infection severity during adult reinfection of neonatally sensitized mice. *J. Virol.* 82:4115–4124.
- Vivier E, Tomasello E, Baratin M, Walzer T, Ugolini S. 2008. Functions of natural killer cells. *Nat. Immunol.* 9:503–510.
- Weiss KA, Christiaansen AF, Fulton RB, Meyerholz DK, Varga SM. 2011. Multiple CD4+ T cell subsets produce immunomodulatory IL-10 during respiratory syncytial virus infection. *J. Immunol.* 187:3145–3154.
- Wiemann K, et al. 2005. Systemic NKG2D down-regulation impairs NK and CD8 T cell responses in vivo. *J. Immunol.* 175:720–729.
- Ziegler SF, Ramsdell F, Alderson MR. 1994. The activation antigen CD69. *Stem Cells* 12:456–465.